Photoelectron spectroscopy and density functional theory studies on the uridine homodimer radical anions

Yeon Jae Ko, Piotr Storoniak, Haopeng Wang, Kit H. Bowen, and Janusz Rak

Citation: J. Chem. Phys. **137**, 205101 (2012); doi: 10.1063/1.4767053
View online: http://dx.doi.org/10.1063/1.4767053
View Table of Contents: http://jcp.aip.org/resource/1/JCPSA6/v137/i20
Published by the American Institute of Physics.

Photoelectron spectroscopy and density functional theory studies on the uridine homodimer radical anions

Yeon Jae Ko,[1,a)] Piotr Storoniak,[2,b)] Haopeng Wang,[1] Kit H. Bowen,[1,b)] and Janusz Rak[2]
[1]*Department of Chemistry, Johns Hopkins University, Baltimore, Maryland 21218, USA*
[2]*Department of Chemistry, University of Gdańsk, Sobieskiego 18, 80-952 Gdańsk, Poland*

(Received 14 September 2012; accepted 28 October 2012; published online 26 November 2012)

We report the photoelectron spectrum (PES) of the homogeneous dimer anion radical of uridine, $(rU)_2^{\bullet-}$. It features a broad band consisting of an onset of ~1.2 eV and a maximum at the electron binding energy (EBE) ranging from 2.0 to 2.5 eV. Calculations performed at the B3LYP/6-31++G** level of theory suggest that the PES is dominated by dimeric radical anions in which one uridine nucleoside, hosting the excess charge on the base moiety, forms hydrogen bonds via its O8 atom with hydroxyl of the other neutral nucleoside's ribose. The calculated adiabatic electron affinities (AEAGs) and vertical detachment energies (VDEs) of the most stable homodimers show an excellent agreement with the experimental values. The anionic complexes consisting of two intermolecular uracil-uracil hydrogen bonds appeared to be substantially less stable than the uracil-ribose dimers. Despite the fact that uracil-uracil anionic homodimers are additionally stabilized by barrier-free electron-induced proton transfer, their relative thermodynamic stabilities and the calculated VDEs suggest that they do not contribute to the experimental PES spectrum of $(rU)_2^{\bullet-}$. © *2012 American Institute of Physics*. [http://dx.doi.org/10.1063/1.4767053]

I. INTRODUCTION

Since Sanche's *et al.*[1] discovery that dry DNA is highly susceptible to degradation by low energy electrons (LEEs), great quantity of data have been collected on damaging action of LEEs to DNA and its components.[2–14] These findings motivated a tremendous interest in electron attachment to nucleobases (NB) since the anions of purines and pyrimidines are perceived as intermediates in the radiation-induced damage of nucleic acids. Initially, it was proposed that such transient anionic states appear as molecular resonances.[3] Indeed, employing electron transmission spectroscopy (ETS), Burrow *et al.*[15] found the negative vertical electron affinities for the four DNA bases. Similarly, most of computational studies in the nineties inferred lack of the gas phase stability of valence-bound (VB) anions as indicated by their computed negative computational adiabatic electron affinities.[16–20]

On the other hand, the gas phase photoelectron spectroscopy (PES)[21,22] and Rydberg electron transfer spectroscopy (RET)[23] experiments revealed that the isolated pyrimidines (uracil, thymine, and cytosine) may trap the excess electron in their dipole field, forming adiabatically stable dipole-bound (DB) anions. Indeed, the CCSD(T)//MP2 (single-point coupled-cluster with single, double and non-iterative triple excitation at the second order Møller-Plesset geometry) adiabatic electron affinity for the DB anion of uracil was calculated to be 0.069 eV.[24] Moreover, small (0.14–0.25 eV) but positive adiabatic electron affinities of uracil and thymine VB anions were later computed with the B3LYP functional and different basis sets augmented with diffuse functions.[25–28] At that level of methodology, the AEA values of cytosine and guanine VB anions were predicted to be around zero[26–28] and significantly negative for adenine (in the range of −0.35 eV to −0.17 eV).[26–28] The most accurate RI-MP2-R12/CCSD(T) value of 0.04 eV for the VB anion of uracil was calculated by Bachorz *et al.*[29] Nevertheless, the vertical electron affinities (VEAs) of all the nucleobases seem to be negative.[25,26,28] The experimental and computational results concerning the electrophilic properties of nucleobases are summarized in several excellent reviews.[30–32]

The well-established fact that the parent valence anions of nucleobases exist in the condensed phase[33] suggests that interactions with the environment support their covalent anionic form. Indeed, the PES experiments of Hendricks *et al.*[34] and Schiedt *et al.*[22] demonstrated a transformation of DB to VB anions of isolated uracil upon even marginal solvation by a single atom of rare gas or water molecule.[34] The conversion of the dipole-bound to valence uracil and thymine anions upon rare gas atom solvation were also observed in the crossed beam RET studies.[35] Similarly, gas phase hydrogen-bonded complexes of nucleobases with various inorganic[36] and organic (alcohols, acids, aminoacids)[37] proton donors were studied both computationally and experimentally. In those systems, the strong thermodynamic stabilization of resulting valence anions was often accompanied by the barrier-free proton transfer.

The hydrogen-bonded Watson-Crick AT[38–42] and GC[40,43–47] base pairs were also shown to form stable valence anions in the gas phase. The influence of stabilizing hydrogen bonds on the electrophilic properties of AT and GC pairs as well as the nucleoside pairs of dAdT and dGdC was discussed in detail by Gu *et al.*[42,47]

The increased stability of nucleobases VB anions in the presence of even a single solvent molecule suggests

[a)]Present address: Rowland Institute at Harvard, 100 Edwin H. Land Blvd., Cambridge, Massachusetts 02142, USA.
[b)]Authors to whom correspondence should be addressed. Electronic addresses: pondros@chem.univ.gda.pl and kbowen@jhu.edu.

that the sugar moiety chemically attached to the NB via N-glycosidic bonding should exert a similar effect. Indeed, the B3LYP/DZP++ calculations pertaining to 2′-deoxyribonucleosides predicted positive electron affinities for all of them.[48] Later on, Stokes *et al.*,[49] employing a combination of infrared desorption, electron photoemission, and gas jet expansion, recorded the anion photoelectron spectra of the nucleoside parent anions of 2′-deoxythymidine$^{\bullet-}$ (dT$^{\bullet-}$), 2′-deoxycytidine$^{\bullet-}$ (dC$^{\bullet-}$), 2′-deoxyadenosine$^{\bullet-}$ (dA$^{\bullet-}$), uridine$^{\bullet-}$ (rU$^{\bullet-}$), cytidine$^{\bullet-}$ (rC$^{\bullet-}$), adenosine$^{\bullet-}$ (rA$^{\bullet-}$), and guanosine$^{\bullet-}$ (rG$^{\bullet-}$). Their measurements proved the appearance of stable valence radical anions of nucleosides in the gas phase. VDEs and AEAs of dT, dC, and dA extracted from the spectra matched quite well those calculated by Richardson *et al.*[48] and by Li *et al.*[50]

The attachment of the phosphate group to a nucleoside, converting it to a nucleotide, further strengthens its tendency to bind an excess electron by ∼0.08 to 0.27 eV, as was concluded by Gu *et al.* at the DFT level.[51]

As to the best of our knowledge, there have been no experimental studies on the parent (intact) anions of the nucleotides in the gas phase except of the report by Stokes *et al.*,[52] concerning adenosine-5′-monophosphate (5′-AMPH) and 2′-deoxyadenosine-5′-monophosphate (5′-dAMPH). The photoelectron spectra revealed that both nucleotides form stable valence-bound radical anions in the gas phase. The computational study by Kobyłecka *et al.* demonstrated that in the anionic (5′-dAMPH)$^{\bullet-}$, the excess electron on a π^* orbital of purine is stabilized by the spontaneous intramolecular proton transfer from the phosphate group.[53]

Non-canonical base pairs such as the homogeneous dimer of U···U commonly occur in RNA molecules that do not transfer sequence information.[54] Tandem U···U base pairs increase the stability of duplexes allowing for the formation of specific, biologically relevant RNA conformations.[54] Herein, employing infrared desorption, electron photoemission, and a gas jet expansion, we were able to generate intact stable radical anionic species, (uridine)$_2^{\bullet-}$, in the gas phase and record its photoelectron spectrum. In order to interpret the measured spectrum, we conducted density functional theory (DFT) calculations. On the basis of the relative stabilities of conceivable complexes and their propensity to attach and detach the excess electron, we have identified species, which dominate under the experimental conditions. The most stable radical anionic homodimer exhibits the arrangement where one monomer (hosting an excess electron on the base moiety) is hydrogen-bonded via O8 to the sugar hydroxyl groups of the other nucleoside. The calculated VDE values for the most thermodynamically favorable structures are in good agreement with the values extracted from the spectrum. A common feature of the investigated anionic structures is uneven charge distribution, which can be perceived as the solvation of the negatively charged nucleoside, with the electron density localized entirely within the base moiety, by the neutral monomer. Surprisingly, the hydrogen-bonded radical anionic complexes utilizing the typical uracil proton-donor N3H center and the proton-acceptor O8, O7 sites are highly unstable in comparison with the structures featuring uracil-ribose interactions. We have also identified radical anionic complexes stabilized by barrier free intermolecular proton transfer between base moieties but, in contrast to our previous studies, such structures are not the lowest energy configurations and, therefore, should not exhibit in the spectrum of (uridine)$_2^{\bullet-}$.

II. METHODS

A. Experimental details

Uridine (rU) radical dimer anions were generated using a novel pulsed infrared desorption-pulsed visible photoemission anion source, which has been described previously.[49,52]

Anion photoelectron spectroscopy (PES) is conducted by crossing beams of mass-selected negative ions and fixed frequency photons followed by energy-analysis the resultant photodetached electrons. This technique is governed by the energy conserving relationship: $h\nu = EBE + EKE$, where $h\nu$ is the photon energy, EBE is the electron binding energy, and EKE is the measured electron kinetic energy.

Low-power infrared laser pulses (1.17 eV/photon) from a Nd:YAG laser were used to desorb neutral uridine from a slowly moving graphite rod, which was thinly coated with the sample. Almost simultaneously, electrons were generated by visible laser pulses (another Nd:YAG laser operated at 532 nm, 2.33 eV/photon) striking a rotating yttrium oxide disk. Since yttrium's work function of ∼2 eV is slightly below the photon energy of the visible laser, low energy electrons were produced, and this process is critical to the formation of intact biomolecular ions. At the same time, a pulsed valve provided a collisionally cooled jet of helium to carry away excess energy and stabilize the resulting parent radical anions. The photoelectron spectrum of the intact uridine dimer radical anions was recorded by crossing a mass-selected beam of (rU)$_2^{\bullet-}$ parent anions with a fixed-frequency photon beam (third Nd:YAG laser operated at 355 nm, 3.49 eV/photon). The resultant photodetached electrons were energy-analyzed using a magnetic bottle energy analyzer with a resolution of 35 meV at EKE = 1 eV.

B. Computational details

We have applied the density functional theory method with Becke's three-parameter hybrid functional (B3LYP)[55–57] and the 6-31++G** basis set.[58,59] The usefulness of the B3LYP/6-31++G** method to describe intra- and intermolecular hydrogen bonds has been demonstrated through comparison with the second order Møller-Plesset (MP2) predictions.[60] The ability of the B3LYP method to predict excess electron binding energies was reviewed and the results were found to be satisfactory for valence-type molecular anions.[61]

All geometries presented here have been fully optimized without geometrical constraints, and the analysis of harmonic frequencies proved that all of them are also geometrically stable (all force constants were positive).

The relative energies, ΔE, and Gibbs free energies, ΔG, of the neutral and anionic complexes are defined with respect to the energy of the most stable neutral or anionic configuration. The stabilization free energies, G_{stab}, of neutral complexes are calculated as a difference between the energy of

the complex and the sum of the energies of fully optimized isolated monomers.

The adiabatic electron affinities, AEA_G, are defined as the Gibbs free energies difference between the neutral and the anion for both species at their fully relaxed geometries. The free energies of the neutral and anionic species result from correcting the relevant values of electronic energies for zero-point vibration terms, thermal contributions to energy, the pV term, and the entropy terms. These terms were calculated in the rigid rotor-harmonic oscillator approximation at $T = 298$ K and $p = 1$ atm.

Electron VDEs—direct observables in photoelectron spectroscopy experiments—were defined as the energy of neutral dimer minus the energy of the anionic dimer at the geometry of the fully relaxed anion.

In the past, calculations at the B3LYP/6-31++G** level[36(a)] for the valence-bound (uracil$\cdots$water)$^-$ clusters was shown to reproduce very well the VDE value extracted from the photoelectron spectrum.[34] For these systems, the B3LYP/6-31++G** approach appeared as good as the MP2/6-31++G(2df,2p)//MP2/6-311++G** level of theory.[62] However, in order to improve our predictions, we corrected the calculated VDE values by −0.15 eV. Introducing such an increment can be justified by juxtaposing the VDE value of 0.75 eV, obtained at the B3LYP/6-31++G** level for isolated valence-bound uracil, with the VDE of 0.60 eV calculated, for this system, at the coupled-cluster level of theory.[29]

All quantum chemical calculations have been carried out with the GAUSSIAN 03[63] and GAUSSIAN 09[64] codes. The pictures of molecules and molecular orbitals and were plotted using the GaussView 4.1 program.[65]

III. RESULTS AND DISCUSSION

A. Photoelectron results

Photoelectron spectrum of the uridine dimer radical anion is presented in Figure 1. The broad peak, indicative of valence-bound anions, results from the vertical photodetachment of the excess electron from a ground vibronic state of mass-selected nucleoside dimer radical anions to the ground vibronic state of the resulting neutrals. The maximal photoelectron intensities correspond to the optimal Franck-Condon overlaps of the vibrational wave functions between anion and neutral ground states. The photoelectron spectrum of $(rU)_2^{\bullet-}$ features an onset at EBE around 1.2 eV and exhibits a broad peak covering the range of ∼1.2–3 eV (see Figure 1) with maximum intensity at the EBE of 2.0–2.5 eV. Thus, the vertical detachment energy (VDE) is in the range of 2.0–2.5 eV, in agreement with our computational result. The electron affinity (EA) is more difficult to determine explicitly. Since there are often vibrational hot bands present in spectra such as these, the threshold EBE energy is probably not exactly equivalent to the value of the EA. As a reasonable approximation, however, one can estimate the EA value as corresponding to the EBE at ∼10% of the rising photoelectron intensity. This puts the value of EA at ∼1.5 eV, in an excellent agreement with the computational value of 1.45 eV.

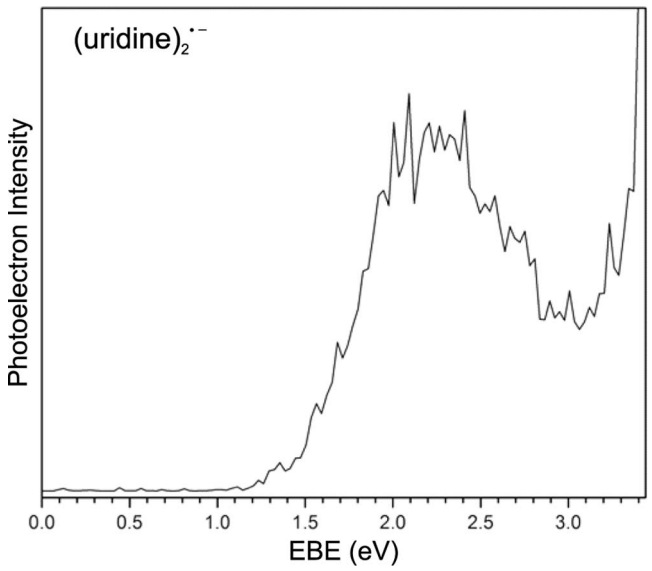

FIG. 1. Photoelectron spectrum of $(uridine)_2^{\bullet-}$ recorded with 3.49 eV photons.

The photoelectron spectrum of the radical anionic uridine monomer ($rU^{\bullet-}$)[49] resembles that of $(rU)_2^{\bullet-}$, but is substantially shifted to lower electron binding energies. Indeed, the $rU^{\bullet-}$ PES exhibits a maximum intensity at the EBE range of ∼1.2–1.6 and an onset at ∼0.7 eV.[49] On the other hand, the photoelectron spectrum of the anionic homodimer form of uracil ($U_2^{\bullet-}$),[66] similarly to $(rU)_2^{\bullet-}$, exhibits a dominant broad peak with the maximum covering almost identical range, 2–2.5 eV, with gradually increasing intensity toward the high electron binding energy (EBE) end of the spectrum, however, its onset falls at a significantly lower EBE (∼0.7 eV).

B. Computational results

The starting geometries of uridine were taken from Leulliot *et al.*,[67] where the complete geometry optimizations of the representative for RNA uridine conformations were performed at the DFT level. We have found the neutral C2′-endo/*anti* monomer to be the most stable while C3′-endo/*anti* to be the least stable at the B3LYP/6-31++G** level of theory and all four considered conformers span a narrow range of 0.7 kcal/mol in terms of both the relative energy and Gibbs free energy (see Table I and Figure 2). Thus, the selection of a

TABLE I. Values of relative electronic energy, free energy (ΔE and ΔG) for the four conformations of the neutral and anion radical uridine, vertical detachment energies (VDEs), and adiabatic electron affinities (AEAs) of anion radical uridine calculated at the B3LYP/6-31++G** level. ΔE, ΔG are given in kcal/mol and AEA_G and VDE in eV.

	Neutrals		Anions			
Conformation	ΔE	ΔG	ΔE	ΔG	AEA_G	VDE
C2′-endo/*anti*	0	0	0	0	0.73	1.62
C2′-endo/*syn*	0.29	1.13	5.09	3.84	0.61	1.21
C3′-endo/*anti*	0.73	0.72	Converges to C2′-endo/*anti*			
C3′-endo/*syn*	0.93	1.39	7.45	5.73	0.54	1.01

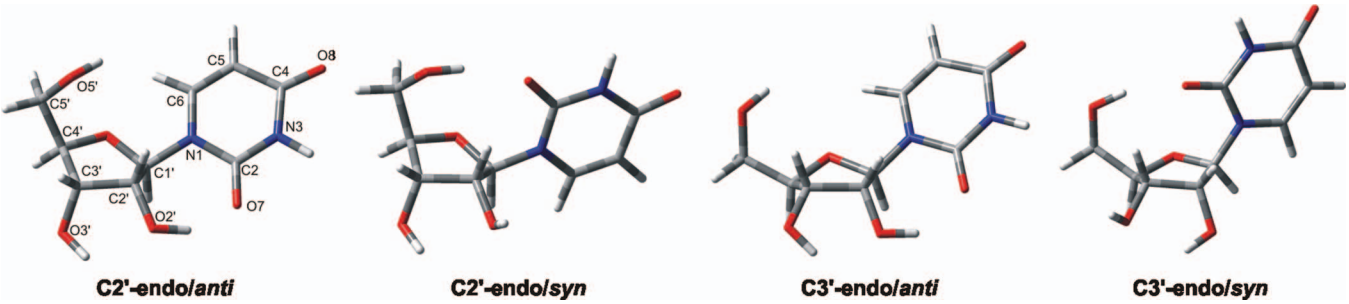

FIG. 2. Neutral conformations of uridine optimized at the B3LYP/6-31++G** level.

monomeric model for further studies by using the stability of the particular neutral conformers does not seem to be justified. However, photoelectron spectrum measured by Stokes *et al.* revealed that the VDE and AEA values of isolated valence-bound uridine amounts to 1.39 and ∼0.7 eV, respectively.[49] Upon re-optimization of the four monomeric uridine conformers listed in Table I as anion radicals, we found out that VDE equal to 1.47 eV (after correction with −0.15 eV) and AEA_G = 0.73 eV for the C2′-endo/*anti* structure remain in good accordance with experimental VDE and AEA of $rU^{\bullet-}$. Moreover, the C2′-endo/*anti* radical anion was also identified as the most stable among the considered anionic structures (see Table I). The next most stable anionic conformer, C2′-endo/*syn,* is separated from C2′-endo/*anti* by as much as 5.1 and 3.8 kcal/mol in terms of E and G, respectively. The calculated VDE and AEA_G values of the C2′-endo/*syn* conformer amount to 1.06 (after correction with −0.15 eV) and 0.61 eV, respectively. Thus, the thermodynamic stability and the electrophilic characteristics of C2′-endo/*syn* do not support the existence of this radical anion in the gas phase.

Noticing that the neutral geometries do not change drastically upon electron attachment (except for C3′-endo/*anti*) and, what is more important, that the relative stability order is the same for both neutrals and anions, we assume that the relative stabilities of neutral uridine conformations in the gas phase may be deduced from the stability of anionic radicals. In view of foregoing, we decided that the C2′-endo/*anti* geometry of neutral uridine is the proper choice for the current study. The fact that the isolated ribose C2′-endo conformation is slightly more stable than C3′-endo[67] also speaks in favor of the C2′-endo/*anti* geometry.

1. Neutral dimer conformations

Uracil nucleoside dimers can be stabilized by hydrogen bonding via proton acceptor sites (O7 or O8) and proton donor sites (N3) of the nucleobases, as well as the OH proton donor groups of the ribose moiety. Figure 3 displays the neutral complexes optimized at the B3LYP/6-31++G** level. All involve the C2′-endo/*anti* conformation of uridine.

There are three conceivable hydrogen-bonded structures involving interactions exclusively among the two uracils. We named them n1, n2, and n3 with the supplementary labeling of the proton acceptor atoms participating in the hydrogen bonding scheme. The complexes n1_O8-O8 (both uracils engage their O8 and N3H atoms) and n3_O7-O7 (both uracils engage the same O7 and N3H centers) are "symmetrical" while the n2_O8-O7 structure features an "asymmetrical" scheme of hydrogen bonds O8···H–N3, O7···H–N3.

Homodimers involving uracil-ribose hydrogen bonding interactions are depicted on the lower half of Figure 3. Upon rotation of uridine with respect to the hydroxyl groups of sugar, we obtained several structures of similar energy. Here, we show only four of these conformers, which were selected to illustrate the most significant geometrical differences within the current hydrogen bonding scheme. These structures are numbered from n4 to n7 and in contrast to the

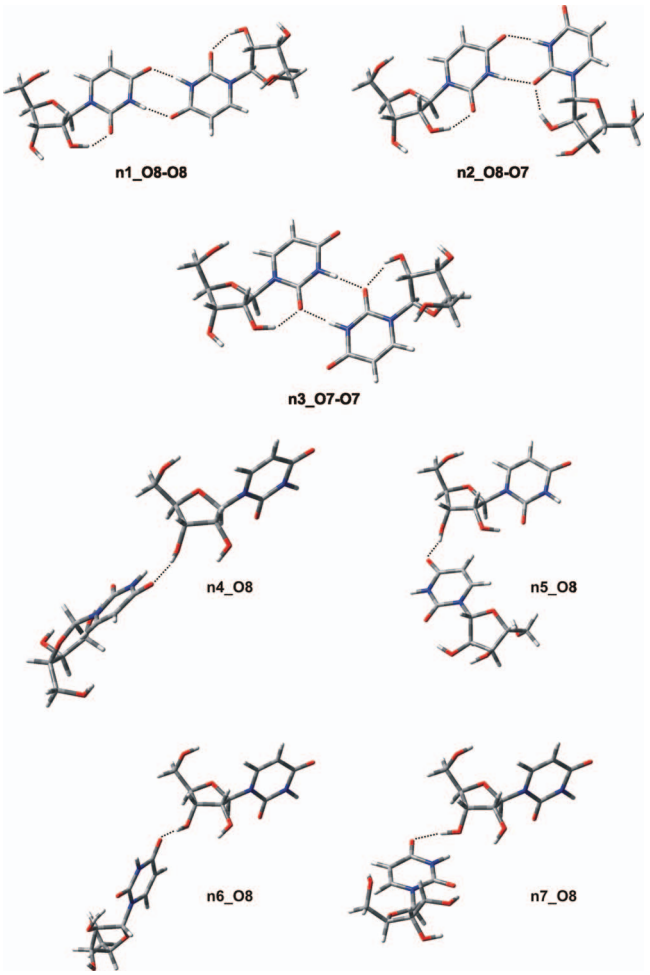

FIG. 3. Structures of neutral uridine dimers optimized at the B3LYP/6-31++G** level.

TABLE II. Values of relative electronic energy and free energy (ΔE and ΔG) with respect to the most stable neutral uridine dimer and stabilization free energies (G_{stab}) of the neutral uridine dimers calculated at the B3LYP/6-31++G** level. All values given in kcal/mol.

Complex	ΔE	ΔG	G_{stab}
n1_O8-O8	0.00	0.00	0.04
n2_O8-O7	2.19	1.13	1.18
n3_O7-O7	3.63	2.46	2.50
n4_O8	6.54	5.04	5.09
n5_O8	7.07	4.52	4.56
n6_O8	7.22	3.54	3.58
n7_O8	7.55	5.45	5.50

previous uracil-uracil bonding motif, only one O8 label is used in the nomenclature since the conformers are stabilized by a single hydrogen bond. The relative energies and Gibbs free energies (ΔE and ΔG) as well as the stabilization enthalpies (G_{stab}) of the neutral uridine homodimers, gathered in Table II are sorted according to their energy values. The G_{stab} values, ranging from 0 to 5.5 kcal/mol (see Table II), suggest that dimerization is not thermodynamically favored.

2. Anions resulting from electron attachment

The fully optimized neutral complexes, described in Sec. III B 1 (see Figure 3), were used as starting points for the investigation of the electrophilic properties of $(rU)_2$. The results of B3LYP/6-31++G** calculations for $(rU)_2^{\bullet-}$ are summarized in Table III and the respective structures are shown in Figure 4. Using the seven neutral parents, we have obtained a large number of anionic geometries as the system under investigation is characterized by a large number of conformational degrees of freedom, particularly the complexes where the nucleosides interact with each other through the sugar moiety (structures a*x*_O8, where $x = 1$–7). Fortunately, most of these conformers lie close to each other on the potential energy surface and exhibit similar electrophilic properties. Thus, the fourteen structures displayed in Figure 4 are the representative geometries of the thoroughly scrutinized conformational space of the uridine homodimer anionic radical complex.

Attachment of the excess electron to the neutral uracil-uracil arrangements (structures n1_O8-O8, n2_O8-O7, and n3_O7-O7) leads to the structures stabilized by two hydrogen bonds, which do not allow for a large change of mutual positions of monomers. Two types of anions are formed in this case–structures that resemble the neutral parent showing similar double hydrogen bonding motifs, and structures where electron-induced proton transfer occurs in one of the two H-bonds (a8_O8-O8-pt, and a9_O8-O7-pt). The proton acceptor site is exclusively the O8 atom, which is not surprising based on the SOMO shapes plotted in Figure 4. The complete lack of the electron density on the O7 atom of uridine makes the O8 atom the only available proton-accepting center within the considered dimers.

As expected from the broad shape of photoelectron spectrum shown in the current report and from previous studies demonstrating that nucleobase anions (and other anionic

TABLE III. Values of relative electronic energy and free energy (ΔE and ΔG) with respect to the most stable uridine homodimer radical anion, stabilization free energies (G_{stab}), vertical detachment energies (VDEs), and adiabatic electron affinities (AEAs) of anion radical uridine homodimers calculated at the B3LYP/6-31++G** level. ΔE, ΔG, and $G_{stab,}$ are given in kcal/mol and AEA_G and VDE in eV.

Complex	ΔE	ΔG	G_{stab}	AEA_G	VDE[a]
a1_O8	0.00	0.00	− 13.43	1.46[b]	2.61 (2.46)
a2_O8	1.69	0.04	− 13.38	1.46[b]	2.45 (2.30)
a3_O8	3.77	0.55	− 12.88	1.44[b]	2.46 (2.31)
a4_O8	4.08	0.20	− 13.23	1.45[b]	2.42 (2.27)
a5_O8	4.10	1.04	− 12.39	1.42[b]	2.43 (2.28)
a6_O8	4.64	0.91	− 12.52	1.42[b]	2.42 (2.27)
a7_O8	4.81	1.32	− 12.10	1.41[b]	2.41 (2.26)
a8_O8-O8-pt	6.73	4.20	− 9.23	1.13[c]	2.69 (2.54)
a9_O8-O7-pt	8.52	5.68	− 7.74	1.11[d]	2.76 (2.61)
a10_O8-O8	9.36	6.12	− 7.30	1.04[c]	1.93 (1.78)
a11_O8-O7	10.41	7.85	− 5.58	1.02[d]	1.96 (1.81)
a12_O8-O8	10.57	5.46	− 7.97	1.07[c]	1.09 (0.94)
a13_O7-O7	15.18	11.34	− 2.08	0.92[e]	1.17 (1.02)
a14_O7-O7	16.63	14.03	0.60	0.81[e]	1.65 (1.50)

[a]In parentheses are given VDE values corrected by −0.15 eV. For details, see Sec. II.
[b]AEA_G calculated from the difference in Gibbs free energies of the neutral structure n6_O8 and the given anionic structure.
[c]AEA_G calculated from the difference in Gibbs free energies of the neutral structure n1_O8-O8 and the given anionic structure.
[d]AEA_G calculated from the difference in Gibbs free energies of the neutral structure n2_O8-O7 and the given anionic structure.
[e]AEA_G calculated from the difference in Gibbs free energies of the neutral structure n3_O7-O7 and the given anionic structure.

DNA/RNA subunits) are thermodynamically stable in the gas phase provided that the solvent molecule is present in the vicinity,[22,34–51] all $(rU)_2^{\bullet-}$ complexes reported here exhibit valence-bound character. Inspection of the anionic wave functions of complexes reveals that in most cases, the excess electron locates on a π^* orbital of uracil of only one of the interacting monomers. Therefore, the dimer structures may be perceived as uridine radical anions solvated by neutral counterparts.

All considered homodimers form adiabatically stable anions as indicated by the AEA_G values in Table III which span the range of 0.81–1.46 eV.

According to the relative stabilities of the anionic radical complexes (Table III), a clear picture emerges that dominating in the gas phase should be the geometries of the a*x*_O8 family, where one of the nucleoside is hydrogen bonded via the O8 atom of its uracil to one or two OH groups of the second nucleoside's sugar (uracil-ribose pattern of interactions). In such geometries, the excess electron is completely localized on the uracil moiety of one nucleoside, which is interacting with the second, neutral monomer via its O8 atom. For the seven most stable structures (a*x*_O8, where $x = 1$–7), the G_{stab} values lie between −13.43 and −12.10 kcal/mol. In contrast to the relatively unstable uracil-ribose n*x*_O8 neutral dimers (characterized by positive G_{stab} values in the range of 3.58 to 5.5 kcal/mol), the corresponding anionic dimers a*x*_O8 exhibit significant stability.

For the most stable geometries, a1_O8 and a2_O8, we have unexpectedly found that the neutral monomers adopt the C2′-endo/*syn* conformation. Additionally, the C3′-endo/*anti*

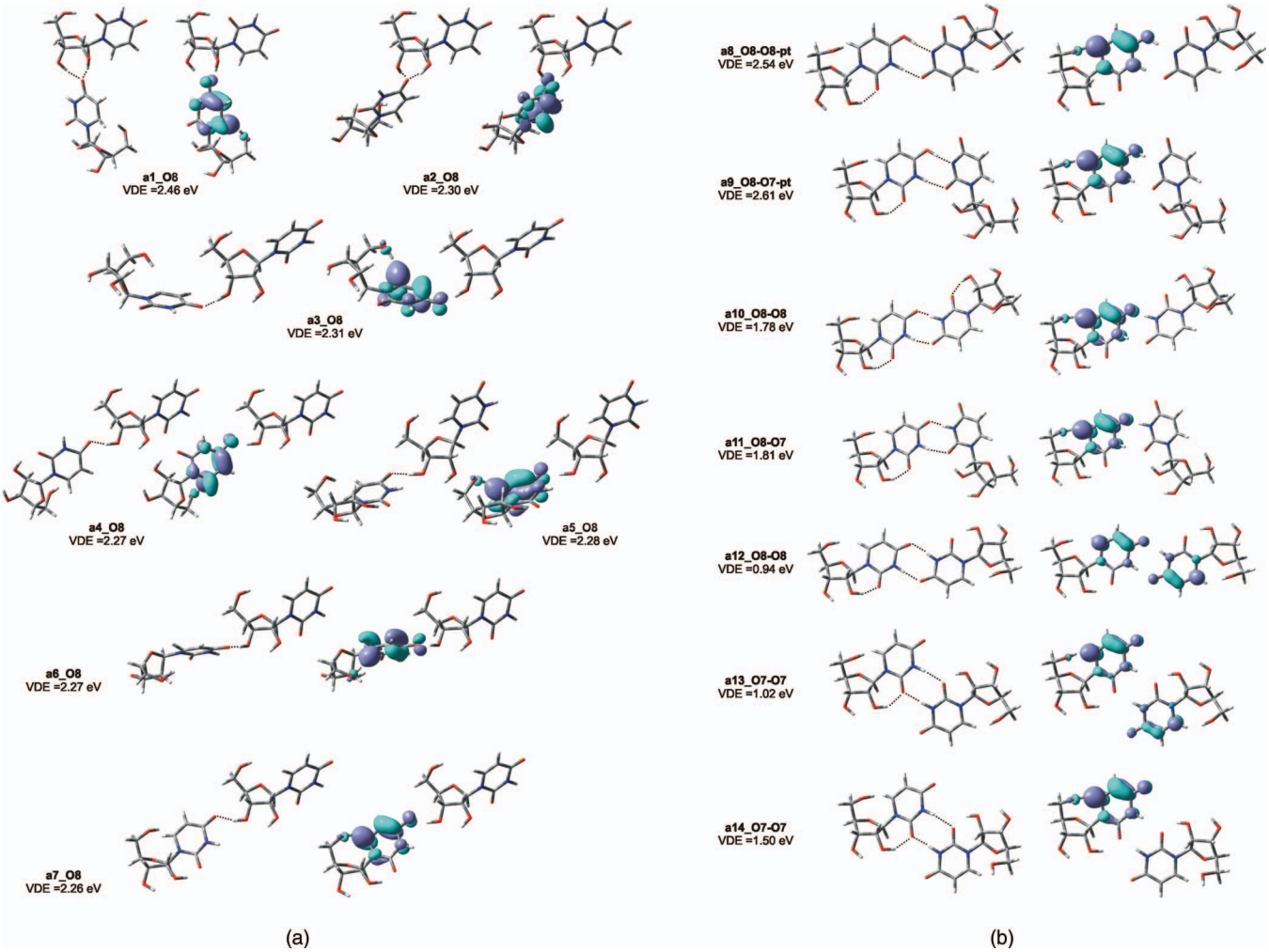

FIG. 4. Structures of anion radical uridine dimers optimized at the B3LYP/6-31++G** level with corresponding VDE values and their singly occupied molecular orbitals plotted with a contour value of 0.05 bohr$^{-3/2}$.

conformer was identified in a5_O8. The four remaining anionic dimers of the ax_O8 family as well as the seven homodimers from the other family, shown in Figure 4, are uniformly composed of the C2′-endo/*anti* monomers. The least stable structure among the a*x*_O8 structures, that is a7_O8, is separated by 4.8 and 1.3 kcal/mol from the most stable a1_O8 in the energy and free energy scale, respectively (see Table III). The calculated VDE values (incremented by −0.15 eV), 2.46 eV for the most stable a1_O8 and 2.26 eV for the least stable a7_O8, agree very well with the broad feature of the PES spectrum at maximum EBE range of 2.0 to 2.5 eV.

The least stable member of "uracil-ribose" family is separated from the next structure (which is a8_O8-O8-pt) by 1.92 and 2.88 kcal/mol in the term of E and G (see Table III), respectively. The anionic a8_O8-O8-pt and a9_O8-O7-pt structures are stabilized by electron-induced intermolecular proton transfer (PT) occurring between the complementary uracil moieties. Based on our earlier experiences with anionic complexes of biomolecules in the gas phase, we expected the PT structures to be the most stable geometries among considered radical anions. However, the data gathered in Table III demonstrate unequivocally that both PT homodimers should not be populated in the gas phase. Despite of the favorable G_{stab} values equal to −9.3 and −7.7 kcal/mol and positive AEA_G's of ∼1.1 eV, both a8_O8-O8-pt and a9_O8-O7-pt are too high on the energy (6.7 and 8.5 kcal/mol, respectively) and free energy scale (4.2 and 5.7 kcal/mol) to compete with any of the a*x*_O8 geometries.

Similarly, the relatively small stabilities for the non-PT "uracil-uracil" anions (a10 to a14 structures; see Table III), suggest that such anionic complexes do not form under the conditions of the photoelectron experiment.

IV. DISCUSSION

The calculations carried out on conceivable neutral homodimers enabled the fourteen anionic $(uridine)_2^{\bullet-}$ structures depicted in Figure 4 to be identified and characterized. The charge distribution of the unpaired electron in uridine homodimers is uneven: one of the two nucleosides accepts the excess electron, which is accompanied by pyrimidine ring distortion, while its counterpart monomer stays neutral. The main part of the excess electron density resides on the C4, C5, and C6 sites of uracil and smaller amounts on the N1, N3, and O8 atoms. An identical shape of the unpaired electron orbital

was found for the isolated 1-methyluracil and non-methylated uracil anions.[29]

Since dimerization is not favorable for the neutral monomers (see positive G_{stab} values gathered in Table II), the formation of anionic radical dimers probably begins with electron capture by a single nucleoside rather than by a neutral dimer. The resulting monomeric anion radical could be subsequently stabilized by dimerization with the neutral uridine. The G_{stab} values predicted for the anionic homodimers (see Table III) are in favor of such a mechanism. Strong stabilization of the $(rU)_2^{\bullet-}$ complexes characterized by the negative G_{stab} and positive AEA_G values results in VDEs much larger than 2 eV. In our previous studies,[36,37,41,53] VDEs close to 2 eV were computed exclusively for the radical anions stabilized by proton transfer (PT). Here, we demonstrated that VDEs above 2 eV can occur for non-PT anions. Moreover, such non-PT complexes turned out to be the most stable anionic geometries (a*x*_O8 family) and therefore should have a dominating contribution to the main PES signal covering the EBEs of 2.26–2.46 eV. On the other hand, the PT-structures were shown to be significantly unstable with respect to the a*x*_O8 geometries, although characterized by similarly high VDEs (~2.5 eV).

The prevailing stability of the a*x*_O8 family with regard to a*x*_O8-O8, a*x*_O7-O7, and a*x*_O8-O7 is surprising given the fact that the uracil-ribose interactions involve a single, O8···HO, or a bifurcated hydrogen bond while each structure featuring a uracil-uracil interaction contains two intermolecular (O8···HN3 or O7···HN3) hydrogen bonds. The intermolecular hydrogen bonds in which the hydroxyl groups of ribose participate are not unusual in biological systems. It was observed that certain conformations of RNA are extraordinarily stable and conserved due to the presence of such inter-strand interactions.[54] What is also important is that the formation of hydrogen bonds involving sugar OH groups may be correlated to the conformational change of sugar puckering from C3′-endo to C2′-endo.[68,69]

The most stable structures, a1_O8 and a2_O8, differ from the other a*x*_O8 ($x = 3$–7) geometries (as well as from the other "uracil-uracil" structures) by the presence of the *syn* conformer. The *syn* orientation of the OH-donating neutral nucleoside enables the bifurcated H-bond between O2′H and O3′H of ribose and the O8 atom of the anionic uridine (both OH···O8 distances are similar to each other and amount to ~1.7 Å; see Figure 4) to be formed in a1_O8 and a2_O8. Both structures are almost identical energetically (free energy difference of 0.04 kcal/mol, difference in G_{stab} equal to 0.05 kcal/mol, and identical AEA_G). Since the thermodynamic characteristics of the a*x*_O8 structures do not vary substantially, one may draw a conclusion that the (uracil)O8···HO(ribose) interaction rather than *syn* or C3′-endo conformation is responsible for the extraordinary stabilization of the excess charge in this family of geometries.

V. SUMMARY

In the present work, we report on the electrophilic properties of uridine homodimers in the gas phase that were characterized with photoelectron spectroscopy and quantum chemistry modeling.

Photoelectron spectrum of uridine homodimer radical anions, $(rU)_2^{\bullet-}$, was registered using infrared desorption/photoemission anion generation and pulsed laser photodetachment. The spectrum exhibits a broad signal with a threshold at ~1.2 eV and a maximum intensity at 2.0–2.5 eV (Figure 1). The shape of photoelectron spectrum of uridine anions ($rU^{\bullet-}$) registered previously resembles that of $(rU)_2^{\bullet-}$. However, dimerization process shifts the $(rU)_2^{\bullet-}$ PES maximum by around 0.8 eV to the higher EBEs when compared to $rU^{\bullet-}$. On the other hand, the photoelectron spectra of $uracil_2^{\bullet-}$ ($U_2^{\bullet-}$) and $(rU)_2^{\bullet-}$ are characterized by the maximum intensity lying within the same EBE range.

The results of our computational studies suggest that formation of the neutral uridine homodimers in the gas phase is thermodynamically improbable while the existence of the highly stable valence radical anions of this dimer is plausibe in agreement with the experimental observations. A common feature of the investigated anionic structures is an uneven charge distribution, which suggests that the negatively charged nucleoside, with the electron density localized entirely within the base moiety, is solvated by a neutral monomer. In the most stable radical anionic homodimer that has a predominant contribution to the PES signal, the nucleoside hosting the excess charge on the base moiety forms a bifurcated hydrogen bond via its O8 atom with two hydroxyl groups of the other neutral nucleoside's ribose. Its calculated VDE of 2.46 eV fits perfectly the VDE measured by PES.

The anionic radical complexes consisting of two intermolecular uracil-uracil hydrogen bonds are substantially less stable than the uracil-ribose dimers. Despite the fact that the uracil-uracil anionic radical homodimers are additionally stabilized by barrier-free electron-induced proton transfer, their relative thermodynamic stabilities and the calculated VDEs suggest that they do not contribute to the experimental PES spectrum of $(rU)_2^{\bullet-}$.

ACKNOWLEDGMENTS

The experimental results reported here are based upon work supported by the National Science Foundation grant to K.H.B. (Grant No. CHE-1111693), and the theoretical parts were supported by the Polish Ministry of Science and Higher Education grant to J.R. (Grant No. DS/8221-4-0140-12). The calculations have been carried out at the Wrocław Center for Networking and Supercomputing (http://www.wcss.wroc.pl) (Grant No. 196) and at the Academic Computer Center in Gdańsk (TASK).

[1] B. Boudaïffa, P. Cloutier, D. Hunting, M. A. Huels, and L. Sanche, Science **287**, 1658 (2000).
[2] B. Boudaïffa, P. Cloutier, D. Hunting, M. A. Huels, and L. Sanche, Radiat. Res. **157**, 227 (2002).
[3] M. A. Huels, B. Boudaïffa, P. Cloutier, D. Hunting, M. A. Huels, and L. Sanche, J. Am. Chem. Soc. **125**, 4467 (2003).
[4] F. Martin, P. D. Burrow, Z. Cai, P. Cloutier, D. Hunting, and L. Sanche, Phys. Rev. Lett. **93**, 068101 (2004).
[5] Y. Zheng, P. Cloutier, D. J. Hunting, L. Sanche, and J. R. Wagner, J. Am. Chem. Soc. **127**, 16592 (2005).
[6] Z. Cai, P. Cloutier, D. Hunting, and L. Sanche, J. Phys. Chem. B **109**, 4796 (2005).

[7]R. Panajotovic, F. Martin, P. Cloutier, D. Hunting, and L. Sanche, Radiat. Res. **165**, 452 (2006).
[8]Y. Zheng, P. Cloutier, D. J. Hunting, J. R. Wagner, and L. Sanche, J. Chem. Phys. **124**, 064710 (2006).
[9]Y. Zheng, J. R. Wagner, and L. Sanche, Phys. Rev. Lett. **96**, 208101 (2006).
[10]Z. Li, Y. Zheng, P. Cloutier, L. Sanche, and J. R. Wagner, J. Am. Chem. Soc. **130**, 5612 (2008).
[11]H. Abdoul-Carime and L. Sanche, Int. J. Radiat. Biol. **78**, 89 (2002).
[12]L. Sanche, Mass Spectrom. Rev. **21**, 349 (2002).
[13]X. Pan, P. Cloutier, D. Hunting, and L. Sanche, Phys. Rev. Lett. **90**, 208102 (2003).
[14]X. Pan and L. Sanche, Phys. Rev. Lett. **94**, 198104 (2005).
[15]K. Aflatooni, G. Gallup, and P. Burrow, J. Phys. Chem. A **102**, 6205 (1998).
[16]N. Oyler and L. Adamowicz, J. Phys. Chem. **97**, 11122 (1993).
[17]N. Oyler and L. Adamowicz, Chem. Phys. Lett. **219**, 223 (1994).
[18]C. Desfrancois, H. Abdoul-Carime, S. Carles, V. Periquet, J. Schermann, D. Smith, and L. Adamowicz, J. Chem. Phys. **110**, 11876 (1999).
[19]D. Smith, J. Smets, Y. Elkadi, and L. Adamowicz, J. Phys. Chem. A **101**, 8123 (1997).
[20]O. Dolgounitcheva, V. Zakrzewski, and J. Ortiz, Chem. Phys. Lett. **307**, 220 (1999).
[21]J. H. Hendricks, S. A. Lyapustina, H. L. de Clercq, J. T. Snodgrass, and K. H. Bowen, J. Chem. Phys. **104**, 7788 (1996).
[22]J. Schiedt, R. Weinkauf, D. Neumark, and E. Schlag, Chem. Phys. **239**, 511 (1998).
[23]C. Desfrançois, H. Abdoul-Carime, and J. Schermann, J. Chem. Phys. **104**, 7792 (1996).
[24]R. A. Bachorz, J. Rak, and M. Gutowski, Phys. Chem. Chem. Phys. **7**, 2116 (2005).
[25]S. Wetmore, R. Boyd, and L. Eriksson, Chem. Phys. Lett. **322**, 129 (2000).
[26]N. Russo, M. Toscano, and A. Grand, J. Comput. Chem. **21**, 1243 (2000).
[27]S. Wesolowski, M. Leininger, P. Pentchev, and H. Schaefer, J. Am. Chem. Soc. **123**, 4023 (2001).
[28]X. Li, Z. Cai, and M. Sevilla, J. Phys. Chem. A **106**, 1596 (2002).
[29]R. A. Bachorz, W. Klopper, and M. Gutowski, J. Chem. Phys. **126**, 085101 (2007).
[30]D. Svozil, P. Jungwirth, and Z. Havlas, Collect. Czech. Chem. Commun. **69**, 1395 (2004).
[31]J. Gu, J. Leszczynski, and H. F. Schaefer, "Interactions of electrons with bare and hydrated biomolecules: From nucleic acid bases to DNA segments," Chem. Rev. (in press).
[32]A. Kumar and M. D. Sevilla, "Radiation effects on DNA: Theoretical investigations of electron, hole and excitation pathways to DNA damage," in *Radiation Induced Molecular Phenomena in Nucleic Acids: A Comprehensive Theoretical and Experimental Analysis (Challenges and Advances in Computational Chemistry and Physics)*, edited by M. Shukla and J. Leszczynski (Springer, 2008), pp. 577–617.
[33]M. Yan, D. Becker, S. Summerfield, P. Renke, and M. D. Sevilla, J. Phys. Chem. **96**, 1983 (1992); M. D. Sevilla, *ibid.* **75**, 626 (1971); M. D. Sevilla, D. Becker, M. Yan, and S. R. Summerfield, *ibid.* **95**, 3409 (1991); M. D. Sevilla and D. Becker, in *Royal Society of Chemistry Specialist Periodical Report, Electron Spin Resonance*, edited by B. C. Gilbert, M. J. Davies, and D. M. Murphy (RSC, Cambridge, 2004), Vol. 19, pp. 243.
[34]J. H. Hendricks, S. A. Lyapustina, H. L. de Clercq, and K. H. Bowen, J. Chem. Phys. **108**, 8 (1998).
[35]C. Desfrançois, V. Periquet, Y. Bouteiller, and J. P. Schermann, J. Phys. Chem. A **102**, 1274 (1998).
[36](a) M. Harańczyk, R. Bachorz, J. Rak, M. Gutowski, D. Radisic, S. T. Stokes, J. M. Nilles, and K. H. Bowen, J. Phys. Chem. B **107**, 7889 (2003); (b) M. Harańczyk, J. Rak, M. Gutowski, D. Radisic, S. T. Stokes, J. M. Nilles, and K. H. Bowen, Isr. J. Chem. **44**, 157 (2004).
[37]M. Harańczyk, J. Rak, M. Gutowski, D. Radisic, S. T. Stokes, and K. H. Bowen, J. Phys. Chem. B **109**, 13383 (2005); M. Harańczyk, I. Dąbkowska, J. Rak, M. Gutowski, J. M. Nilles, S. T. Stokes, D. Radisic, and K. H. Bowen, *ibid.* **108**, 6919 (2004); K. Mazurkiewicz, M. Harańczyk, M. Gutowski, J. Rak, D. Radisic, S. N. Eustis, D. Wang, and K. H. Bowen, J. Am. Chem. Soc. **129**, 1216 (2007); K. Mazurkiewicz, M. Haranczyk, P. Storoniak, M. Gutowski, J. Rak, D. Radisic, S. N. Eustis, D. Wang, and K. H. Bowen, Chem. Phys. **342**, 215 (2007); M. Gutowski, I. Dąbkowska, J. Rak, S. Xu, J. M. Nilles, D. Radisic, and K. H. Bowen, Eur. Phys. J. D **20**, 431 (2002); I. Dąbkowska, J. Rak, M. Gutowski, J. M. Nilles, D. Radisic, and K. H. Bowen, J. Chem. Phys. **120**, 6064 (2004); I. Dąbkowska, J. Rak, M. Gutowski, D. Radisic, S. T. Stokes, J. M. Nilles, and K. H. Bowen, Phys. Chem. Chem. Phys. **6**, 4351 (2004).
[38]N. A. Richardson, S. S. Wesolowski, and H. F. Schaefer, J. Phys. Chem. B **107**, 848 (2003).
[39]I. Al-Jihad, J. Smets, and L. Adamowicz, J. Phys. Chem. A **104**, 2994 (2000).
[40]A. Kumar, M. Knapp-Mohammady, P. C. Mishra, and S. Suhai, J. Comput. Chem. **25**, 1047 (2004).
[41]D. Radisic, K. H. Bowen, I. Dąbkowska, P. Storoniak, J. Rak, and M. Gutowski, J. Am. Chem. Soc. **127**, 6443 (2005).
[42]J. Gu, Y. Xie, and H. F. Schaefer, J. Phys. Chem. B **109**, 13067 (2005).
[43]A.-O. Colson, B. Besler, D. M. Close, and M. D. Sevilla, J. Phys. Chem. **96**, 661 (1992).
[44]J. Smets, A. F. Jalbout, and L. Adamowicz, Chem. Phys. Lett. **342**, 342 (2001).
[45]X. Li, Z. Cai, and M. D. Sevilla, J. Phys. Chem. B **105**, 10115 (2001).
[46]N. A. Richardson, S. S. Wesolowski, and H. F. Schaefer III, J. Am. Chem. Soc. **124**, 10163 (2002).
[47]J. Gu, Y. Xie, and H. F. Schaefer III, J. Chem. Phys. **127**, 155107 (2007).
[48]N. A. Richardson, J. Gu, S. Wang, Y. Xie, and H. F. Schaefer III, J. Am. Chem. Soc. **126**, 4404 (2004).
[49]S. T. Stokes, X. Li, A. Grubisic, Y. J. Ko, and K. H. Bowen, J. Chem. Phys. **127**, 084321 (2007).
[50]X. Li, L. Sanche, and M. D. Sevilla, Radiat. Res. **165**, 721 (2006).
[51]J. Gu, Y. Xie, and H. F. Schaefer, Nucleic Acids Res. **35**, 5165 (2007).
[52]S. T. Stokes, A. Grubisic, X. Li, Y. J. Ko, and K. H. Bowen, J. Chem. Phys. **128**, 044314 (2008).
[53]M. Kobyłecka, J. Gu, J. Rak, and J. Leszczynski, J. Chem. Phys. **128**, 044315 (2008).
[54]S. E. Lietzke, C. L. Barnes, J. A. Berglund, and C. E. Kundrot, Structure **4**, 917 (1996).
[55]A. D. Becke, Phys. Rev. A **38**, 3098 (1988).
[56]A. D. Becke, J. Chem. Phys. **98**, 5648 (1993).
[57]C. Lee, W. Yang, and R. G. Parr, Phys. Rev. B **37**, 785 (1988).
[58]R. Ditchfield, W. J. Hehre, and J. A. Pople, J. Chem. Phys. **54**, 724 (1971).
[59]W. J. Hehre, R. Ditchfield, and J. A. Pople, J. Chem. Phys. **56**, 2257 (1972).
[60]T. van Mourik, S. L. Price, and D. C. Clary, J. Phys. Chem. A **103**, 1611 (1999).
[61]J. C. Rienstra-Kiracofe, G. S. Tschumper, and H. F. Schaefer, Chem. Rev. **102**, 231 (2002).
[62]O. Dolgounitcheva, V. Zakrzewski, and J. Ortiz, J. Phys. Chem. A **103**, 7912 (1999).
[63]M. J. Frisch, G. W. Trucks, H. B. Schlegel *et al.*, GAUSSIAN 03, Revision B.05, Gaussian, Inc., Pittsburgh, PA, 2003.
[64]M. J. Frisch, G. W. Trucks, H. B. Schlegel *et al.*, GAUSSIAN 09, Revision B.01, Gaussian, Inc., Pittsburgh, PA, 2010.
[65]R. Dennington II, T. Keith, J. Millam, K. Eppinnett, W. Lee Hovell, and R. Gilliland, GAUSSVIEW, Version 3.09, Semichem, Inc., Shawnee Mission, KS, 2003.
[66]Y. J. Ko, H. Wang, R. Cao, D. Radisic, S. N. Eustis, S. T. Stokes, S. Lyapustina, S. X. Tian, and K. H. Bowen, Phys. Chem. Chem. Phys. **12**, 3535 (2010).
[67]N. Leulliot, M. Ghomi, G. Scalmani, and G. Berthier, J. Phys. Chem. A **103**, 8716 (1999).
[68]M. Chastain and I. Tinoco, Jr., Biochemistry **32**, 14220 (1993).
[69]R. F. Setlik, M. Shibata, R. H. Sarma, M. H. Sarma, A. L. Kazim, R. L. Ornstein, T. B. Tomasi, and R. J. Rein, J. Biomol. Struct. Dyn. **13**, 515 (1995).